Journal of Applied Toxicology

WILEY

Journal of AppliedToxicology

RESEARCH ARTICLE

Hepato-Cardiac Axis in Epirubicin Toxicity: Role of Kynurenine Pathway and N-Acetylcysteine Antioxidant Intervention

Ebru Afşar[1] | Mehmet Öz[2] | Işıl Eranıl[3]

[1]Department of Biochemistry, Faculty of Dentistry, Cappadocia University, Nevşehir, Turkey | [2]Department of Physiology, Faculty of Medicine, Aksaray University, Aksaray, Turkey | [3]Department of Medical Services and Techniques, Cappadocia Vocational School, Cappadocia University, Nevşehir, Turkey

Correspondence: Ebru Afşar (ebru.afsar@kapadokya.edu.tr; ebrukiracc@gmail.com)

Received: 27 November 2025 | **Revised:** 23 January 2026 | **Accepted:** 29 January 2026

Keywords: cardiotoxicity | epirubicin | kynurenine pathway | N-acetylcysteine

ABSTRACT

Epirubicin (EPI) is a widely used chemotherapeutic agent; however, its clinical utility is limited by severe side effects, particularly the production of reactive oxygen species (ROS). Among these, cardiotoxicity is one of the most critical issues, and it is worsened by impaired hepatic clearance resulting from liver dysfunction. This study aimed to investigate molecular changes induced by EPI in the liver within the kynurenine pathway (KP), their possible contribution to cardiotoxicity, and the protective effects of N-acetylcysteine (NAC). Rats received intraperitoneal injections of 50 or 300 mg/kg NAC, followed 1 h later by 9.6 mg/kg EPI. Tryptophan (Trp), kynurenine (Kyn), kynurenic acid (KYNA), quinolinic acid (QA), kynureninase, and kynurenine 3-monooxygenase (KMO) levels in the liver and cleaved caspase-3 levels in the liver and heart tissue were measured using ELISA. Hepatic and cardiac total antioxidant status (TAS) and total oxidant status (TOS) were determined using a colorimetric method. Plasma levels of aspartate aminotransferase (AST), alanine aminotransferase (ALT), creatine kinase (CK), creatine kinase–MB isoenzyme (CK-MB), high-density lipoprotein (HDL), low-density lipoprotein (LDL), total cholesterol (T-chol), and triglyceride (TG) were analyzed with a clinical biochemistry analyzer. Cardiac morphology was examined using hematoxylin–eosin staining. EPI administration was associated with increases in plasma CK-MB, the AST/ALT ratio, LDL, T-chol, and TG, with these increases partially attenuated by NAC treatment. Hepatic levels of Trp, QA, and KMO were positively correlated with plasma CK-MB and the AST/ALT ratio. Additionally, EPI appeared to increase oxidative stress in heart tissue and induce morphological changes. At the same time, NAC treatment was associated with partial improvement in these parameters, suggesting that alterations in the hepatic KP may be linked to possible cardiac involvement. Our findings suggest that EPI-induced alterations in hepatic KP may impair hepatic clearance, and NAC administration may provide partial protection, warranting further investigation of a possible hepato-cardiac interaction.

1 | Introduction

Epirubicin (EPI) is widely used in chemotherapy for various types of cancer (Petit et al. 2020). It exerts its anticancer effects by inhibiting cancer cell proliferation, inhibiting topoisomerase activity, and generating reactive oxygen species (ROS), which also contribute to its side effects (Alves et al. 2016; Kebieche et al. 2009; Fabbi et al. 2015). The use of anthracyclines is restricted by dose-related cardiotoxicity, which initially manifests as asymptomatic cardiac dysfunction and may potentially progress to congestive heart failure (Fabbi et al. 2015). More importantly, the liver plays a crucial role in the elimination of anthracyclines from the body, and toxicity from these drugs can be particularly severe in patients with impaired liver function

(Kebieche et al. 2009; Twelves et al. 1989). Therefore, understanding the molecular changes induced by these drugs in the liver may provide crucial insights for preventing cardiotoxicity.

In recent years, the kynurenine pathway (KP) and its metabolites have been recognized for their involvement in various pathophysiological processes in liver diseases (Tan et al. 2025). In response to inflammatory signals and oxidative stress, the KP is activated by the enzyme indoleamine-2,3-dioxygenase-1 (IDO1), leading to decreased L-tryptophan (L-Trp) levels and increased kynurenine (Kyn) levels. Subsequently, Kyn is converted to KP metabolites through three distinct pathways: conversion to kynurenic acid (KYNA) by kynurenine aminotransferase (KAT); conversion to anthranilic acid by kynureninase and subsequently to quinolinic acid (QA); or conversion to 3-hydroxykynurenine (3-HK) by kynurenine 3-monooxygenase (KMO). Wang et al. (2021) demonstrated that KP activation and KYNA upregulation were implicated in chemotherapeutic-induced intestinal damage. Additionally, Kyn is a ligand for the aryl hydrocarbon receptor (AhR), as reported by Bekki et al. AhR plays a pivotal role in breast cancer development by suppressing apoptosis (Bekki et al. 2015). Collectively, these findings indicate that KP activity is altered during cancer progression and in response to chemotherapeutic treatments. Investigation of EPI-induced changes in KP may contribute to a better understanding of the pathogenesis of EPI-associated hepatic and cardiotoxicity.

N-acetylcysteine (NAC) is a compound recognized as a multitarget drug and dietary supplement with antioxidant and anti-inflammatory properties. NAC also helps prevent oxidative stress and protects against cell damage (Berk et al. 2014; Blanco-Ayala et al. 2020; Ayala et al. 2021). However, the effect of NAC supplementation on the hepatic KP and its potential impact on EPI-mediated toxicity have not been previously studied. Therefore, in the present study, the effects of EPI on the hepatic KP and related biochemical parameters, as well as the potential modulatory role of NAC supplementation on these alterations, were comprehensively investigated.

2 | Materials and Methods

2.1 | Animals and Experimental Design

All experimental protocols were conducted on male albino Wistar rats, aged 3 months and weighing 200–300 g, in accordance with the standards established by the Institutional Animal Care and Use Committee at Aksaray University (2025/07-49). The study used albino rats obtained from the Aksaray University Animal Care Unit. Rats were provided with food and tap water ad libitum, and the animals were housed in polycarbonate cages under standard conditions (23°C ± 1°C and 50% ± 5% humidity) with a 12:12-h light–dark cycle at all times.

The experimental design is shown in Figure 1. Animals were randomly assigned to five groups ($n = 6$ for each group). The EPI-injected group (EPI group) received an intraperitoneal (i.p.) saline injection, followed by an i.p. EPI (9.6 mg/kg) injection 1 h later. The NAC-received group (NAC group) received 300 mg/kg NAC by i.p. injection, followed by saline injection 1 h later. The EPI and NAC groups received either 50 mg/kg NAC (ENAC-50 group) or 300 mg/kg NAC (ENAC-300 group) and, 1 h later, were administered an i.p. EPI injection. The control group (CON) received saline injections twice at 1-h intervals. Five days later,

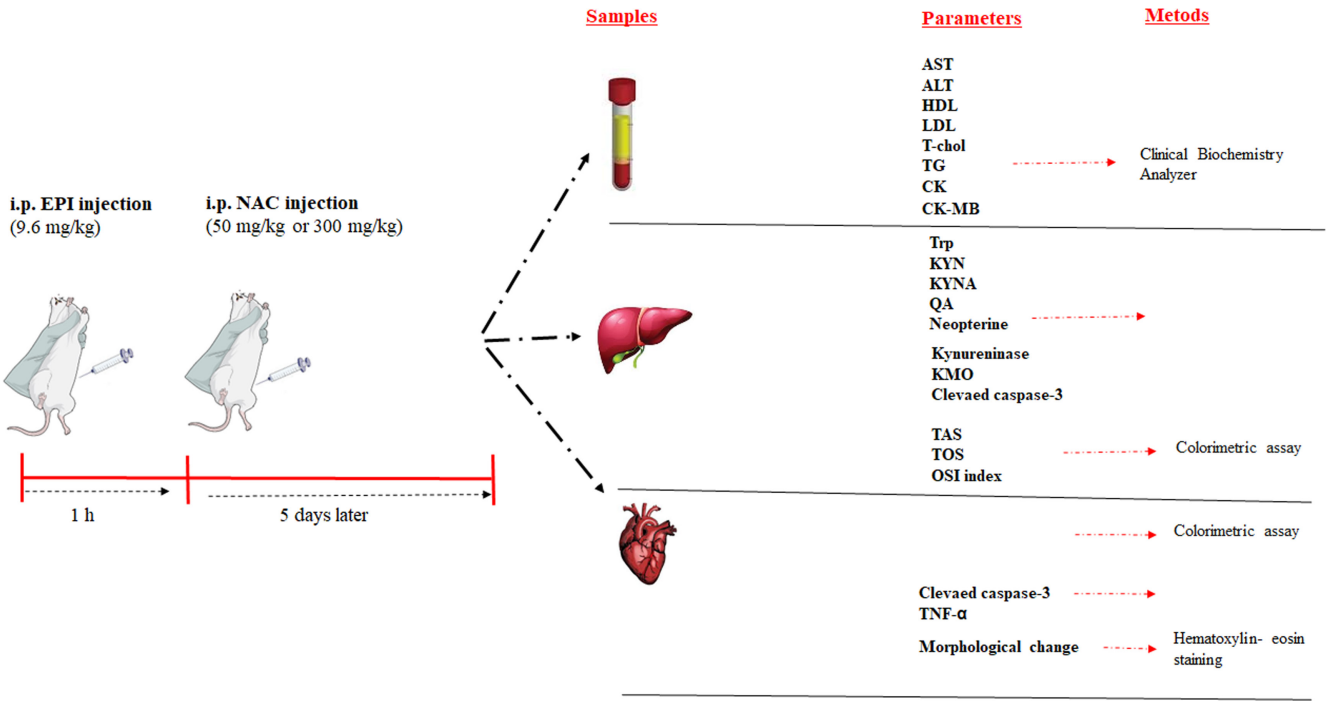

FIGURE 1 | Experimental design. Abbreviations: ALT, alanine aminotransferase; AST, aspartate aminotransferase; CK, creatine kinase; CK-MB, creatine kinase–MB isoenzyme; HDL, high-density lipoprotein; IDO, enzyme indoleamine-2,3-dioxygenase; KMO, Kyn 3-monooxygenase; Kyn, kynurenine; KYNA, kynurenic acid; LDL, low-density lipoprotein; OSI, oxidative stress index; QA, quinolinic acid; TAS, total antioxidant status; T-chol, total cholesterol; TG, triglyceride; TOS, total oxidant status; Trp, tryptophan.

the rats were anesthetized i.p. with a mixture of ketamine (80 mg/kg) and xylazine hydrochloride (5 mg/kg) before being sacrificed. Sigma-Aldrich (St. Louis, MO, USA) supplied the EPI and NAC. Plasma samples were separated by centrifugation at 1500 × g for 15 min. The examined tissues were homogenized in cold phosphate-buffered saline (PBS) at a 1:9 (w/v) buffer-to-tissue ratio. Additionally, body weights of the animals were measured at the beginning and at the end of the experimental period to assess weight loss.

2.1.1 | Determination of Experimental EPI and NAC Doses

We used a 9.6 mg/kg EPI dose for animals, which corresponds to the commonly administered dose for chemotherapy in patients at 60 mg/m^2 (Dobbs et al. 2003; Dobbs et al. 1994; Devaleriola 1994). We used lower (50 mg/kg) and higher (300 mg/kg) doses of NAC administration, which have been beneficial (Sabbaghziarani et al. 2024; Kalimeris et al. 2016), in the present study to investigate the dose-dependent effects in the livers of EPI-treated rats.

2.2 | Plasma Biochemical Parameters

The plasma samples were analyzed using a colorimetric method (Fully Automatic Clinical Biochemistry Analyzer, Mindray BS400), measuring the levels of aspartate aminotransferase (AST), alanine aminotransferase (ALT), high-density lipoprotein (HDL), low-density lipoprotein (LDL), total cholesterol (T-chol), total triglyceride (TG), creatine kinase (CK), and creatine kinase–MB isoenzyme (CK-MB).

2.3 | Oxidative Stress–Related Parameters and KP-Related Parameters

Total antioxidant status (TAS) and total oxidant status (TOS) were measured in liver and heart tissues using a colorimetric test according to the manufacturer's instructions. The oxidative stress index (OSI) was calculated as follows: OSI (arbitrary units) = TOS (μmol H_2O_2 equivalent/L)/TAS (μmol Trolox equivalent/L) (Ozturk et al. 2011). Tryptophan (Trp), Kyn, KYNA, QA, KMO, kynureninase, and neopterin levels were evaluated in liver tissue; cleaved caspase-3 levels in liver and heart tissues; and tumor necrosis factor-alpha (TNF-α) in heart tissue using enzyme-linked immunosorbent assay (ELISA) according to the manufacturer's instructions. Also, the Kyn/Trp ratio (KTR) is calculated to define IDO activity. TAS, TOS, and ELISA measurements in liver and heart tissues were performed using the resulting supernatants obtained after homogenization and centrifugation (1000 × g for 5 min at 4°C) of the tissues, according to the manufacturer's instructions.

The catalog numbers and measurement ranges of the assay kits used were as follows: Trp (E2630Ra, 10–2000 ng/L), Kyn (E12003Ra, 0.2–200 ng/L), KYNA (E2527Ra, 3.75–240 ng/mL), QA (EA0055Ge, 0.13–8 ng/mL), KMO (E2127Ra, 0.1–100 ng/L), kynureninase (E1183Ra, 0.3–90 ng/mL), neopterin (E0958Ra, 0.05–30 nmol/L), cleaved caspase-3 (E2444Ra, 20–6000 ng/L), and TNF-α (E0764Ra, 5–1000 ng/L), all obtained from Bioassay Technology Laboratory (BT Lab, Shanghai, China). TAS (RL007, 0.01–4.00 mmol Trolox equivalent/L) and TOS (RL0024, 0.2–80 μmol H_2O_2 equivalent/L) were measured using kits from Rel Assay Diagnostics (Gaziantep, Türkiye).

2.3.1 | Protein Measurements

Protein concentrations were determined at 595 nm using a modified Bradford assay with Coomassie Plus reagent, employing bovine serum albumin as a standard (Pierce Chemical Company, Rockford, IL, USA) (Bradford 1976).

2.4 | Histopathologic Examinations of Cardiac Tissue

Cardiac tissues were preserved in 10% paraformaldehyde and examined in 5- to 6-μm-thick sections by hematoxylin–eosin (H&E) staining and light microscopy (Zeiss 305, Germany) (Periyanayagam et al. 2015; Dur et al. 2016).

2.5 | Statistical Analysis

Statistical analyses of the obtained data were conducted using SPSS 23.0 (SPSS, Chicago, IL, USA) for Windows. Biochemical parameters were analyzed with a one-way analysis of variance (ANOVA) followed by the Tukey post hoc test for normally distributed variables and a Kruskal–Wallis test followed by the Mann–Whitney *U* test for non-normally distributed variables. Results are presented as the mean ± SEM. A p value of less than 0.05 was deemed statistically significant. Pearson's correlation analysis was used to assess the relationship between the results.

3 | Results

3.1 | Plasma Biochemistry Parameters

As shown in Table 1, the AST levels in the EPI group were markedly higher compared to the CON and ENAC-50 groups and were significantly higher than the NAC group ($p = 0.010$) and the ENAC-300 group ($p = 0.008$). The ALT levels in the NAC, ENAC-50, and ENAC-300 groups were lower than in the CON group ($p = 0.50$, $p = 0.011$, and $p = 0.001$, respectively). ALT levels were markedly lower in the ENAC-300 group than in the EPI group. However, this decreasing trend did not reach significant levels. Also, the AST/ALT ratio of the EPI group was significantly higher than that of the CON group ($p = 0.001$), and the AST/ALT ratio of the ENAC-50 and ENAC-300 groups was significantly lower than that of the EPI group ($p = 0.016$, $p = 0.001$). No difference was observed between groups in plasma HDL levels. LDL levels in the EPI group were significantly higher than in the CON, NAC, ENAC-50, and ENAC-300 groups ($p = 0.001$, $p = 0.001$, $p = 0.004$, and $p = 0.001$, respectively). The TG levels in the EPI group were significantly higher than in the CON, ENAC-50, and ENAC-300 groups ($p = 0.010$, $p = 0.037$, and $p = 0.004$, respectively).

TABLE 1 | Evaluation of changes in biochemical parameters between groups.

	CON	NAC	EPI	ENAC-50	ENAC-300
AST (U/L)	214.4 ± 16.9	176.5 ± 16.5	251.7 ± 15.3	217.2 ± 11.5	175.0 ± 11.3$^{\#\#}$
ALT (U/L)	68.9 ± 4.4	55.2 ± 4.1*	57.1 ± 1.5	52.1 ± 2.0*	44.8 ± 2.8***
AST/ALT	3.19 ± 0.89	2.84 ± 0.18	4.77 ± 0.09***	3.83 ± 0.20$^{\#}$	3.37 ± 0.30$^{\#\#\#}$
HDL (mg/dL)	40.0 ± 2.2	40.0 ± 2.0	39.7 ± 0.8	38.5 ± 2.1	39.7 ± 1.5
LDL (mg/dL)	10.7 ± 0.8	10.4 ± 0.5	14.7 ± 0.3**	11.3 ± 0.6$^{\#\#}$	9.7 ± 0.3$^{\#\#\#}$
TG (mg/dL)	55.8 ± 1.7	55.8 ± 11.6	75.1 ± 7.1*	55.8 ± 6.2$^{\#}$	47.6 ± 1.8$^{\#\#}$
T-chol (mg/dL)	62.9 ± 2.1	65.0 ± 3.3	75.8 ± 2.8*	72.1 ± 4.5	58.0 ± 2.3$^{\#\#\varepsilon}$
CK (U/L)	1872 ± 175	1177 ± 131**	1201 ± 51**	997 ± 98***	811 ± 14.8***
CK-MB (U/L)	753 ± 45	814 ± 44	949 ± 72	672 ± 61$^{\#}$	536 ± 57$^{\#\#\#}$
Change in body weight (g)	7.67 ± 1.667	7.50 ± 5.993	−21.33 ± 2.741**	−10.67 ± 4.499*	−14.17 ± 5.375**

Note: Statistical analysis was performed using a one-way analysis of variance (ANOVA) followed by the Tukey post hoc test for the analysis of AST, ALT, AST/ALT ratio, HDL, LDL, CK, CK-MB, and change in body weight levels and a Kruskal–Wallis one-way ANOVA on ranks. All pairwise multiple comparison procedures were performed using the Mann–Whitney *U* test for the analysis of TG and T-chol levels. All values are mean ± SEM. $n = 6$ for each group.
Abbreviations: ALT, alanine aminotransferase; AST, aspartate aminotransferase; CK, creatine kinase; CK-MB, creatine kinase–MB isoenzyme; CON, control; ENAC-50, EPI + NAC (50 mg/kg); ENAC-300, EPI + NAC (300 mg/kg); EPI, epirubicin; HDL, high-density lipoprotein; LDL, low-density lipoprotein; NAC, N-acetylcysteine; T-chol, total cholesterol; TG, triglyceride.
*$p < 0.05$ vs. CON.
**$p < 0.01$ vs. CON.
***$p < 0.001$ vs. CON.
$^{\#}p < 0.05$ vs. EPI.
$^{\#\#}p < 0.001$ vs. EPI.
$^{\#\#\#}p < 0.000$ vs. EPI.
$^{\#\#\varepsilon}p < 0.05$ vs. ENAC-50.

T-chol levels in the EPI group were significantly higher compared to the CON and ENAC-300 groups ($p = 0.016$, $p = 0.004$). Additionally, in the ENAC-300 group, the values were lower compared to the ENAC-50 group ($p = 0.025$). CK levels in the CON group were significantly higher compared to the NAC, EPI, ENAC-50, and ENAC-300 groups ($p = 0.001$, $p = 0.002$, $p = 0.001$, and $p = 0.001$, respectively). NAC administration decreased CK levels in the ENAC-50 and ENAC-300 groups; however, this trend did not reach statistical significance. Additionally, CK-MB levels increased markedly in the EPI group compared to the CON group; however, this trend did not reach statistical significance. NAC administration significantly reduced CK-MB levels in the ENAC-50 and ENAC-300 groups when compared to the EPI group ($p = 0.016$, $p = 0.001$).

Additionally, animals in the EPI group experienced a significant weight loss compared with the CON and NAC groups ($p = 0.001$, $p = 0.001$). Weight loss was attenuated in the ENAC-50 and ENAC-300 groups; however, this reduction did not reach statistical significance, and body weight remained significantly lower than that of the CON and NAC groups ($p = 0.047$, $p = 0.013$; $p = 0.049$, $p = 0.014$).

3.2 | Hepatic Oxidative Stress and Apoptosis-Related Parameters

Table 2 shows the results of oxidative stress–related parameters in the liver. The liver TAS levels were not different between groups. The liver TOS levels were significantly higher in the EPI group compared to the CON and ENAC-300 groups ($p = 0.002$, $p = 0.018$). The liver OSI levels were higher in the EPI, ENAC-50, and ENAC-300 groups than in the CON group ($p = 0.004$, $p = 0.037$, $p = 0.004$). Also, the OSI levels tended to be lower in the ENAC-50 group than in the EPI group and were significantly lower than in the ENAC-300 group ($p = 0.055$, $p = 0.037$). Cleaved caspase-3 levels showed a nonsignificant increase in the EPI group compared to the CON group ($p = 0.077$), whereas they were significantly reduced in the ENAC-50 group compared to the EPI group ($p = 0.011$). Neopterin levels were significantly higher in the EPI group compared to the CON, ENAC-50, and ENAC-300 groups ($p = 0.016$, $p = 0.006$, and $p = 0.037$, respectively).

3.3 | Heart Oxidative Stress and Apoptosis-Related Parameters

Table 2 shows the results of oxidative stress–related parameters in the heart. TAS levels reduced in the EPI group compared to the CON group, significantly increased compared to the ENAC-50, and markedly increased compared to the ENAC-300 group ($p = 0.004$, $p = 0.006$, $p = 0.78$). TOS levels were higher in the EPI group than in the CON and NAC groups ($p = 0.001$, $p = 0.004$). Also, TOS levels decreased in the ENAC-50 group compared to the EPI group ($p = 0.004$). OSI levels were higher in the EPI group than in the CON, ENAC-50, and ENAC-300 groups ($p = 0.004$, $p = 0.010$, and $p = 0.016$, respectively). TNF-α levels were higher in the EPI group compared to the CON, NAC, ENAC-50, and ENAC-300 groups ($p = 0.001$, $p = 0.001$, $p = 0.001$, and $p = 0.001$, respectively). Cleaved caspase-3 levels were lower in the EPI group than in

TABLE 2 | Evaluation of oxidative stress–related parameters between groups.

	CON	NAC	EPI	ENAC-50	ENAC-300
Liver TAS levels (μmol Trolox/g protein)	0.105 ± 0.01	0.077 ± 0.00	0.097 ± 0.01	0.108 ± 0.009	0.09 ± 0.015
Liver TOS levels (μmol H_2O_2 Eq/g protein)	2.11 ± 0.13	3.75 ± 0.85	5.38 ± 0.52**	3.8 ± 0.48	2.74 ± 0.51#
Liver OSI levels (arbitrary units)	23.60 ± 2.89	49.15 ± 12.09	52.95 ± 9.56**	36.12 ± 3.705*	55.02 ± 5.77**ε
Cleaved caspase-3 (ng/g protein)	124.59 ± 16.0	145.27 ± 8.4	181.18 ± 17.5	106.35 ± 18.6#	139.14 ± 9.3
Neopterin (nmol/g protein)	0.131 ± 0.025	0.157 ± 0.020	0.267 ± 0.05*	0.119 ± 0.020##	0.145 ± 0.021#
Heart cleaved caspase-3 (ng/g protein)	292.698 ± 46.942	289.198 ± 45.221	253.997 ± 31.687	298.761 ± 21.793	295.193 ± 25.761
Heart TAS levels (μmol Trolox/g protein)	0.247 ± 0.019	0.263 ± 0.135	0.105 ± 0.003**	0.145 ± 0.009**##	0.127 ± 0.012#
Heart TOS levels (μmol H_2O_2 Eq/g protein)	2.984 ± 0.203	3.156 ± 0.151	4.694 ± 0.344**##	3.474 ± 0.345#	3.875 ± 0.400
Heart OSI levels (arbitrary units)	12.350 ± 1.213	34.699 ± 14.147	44.558 ± 2.710**	27.326 ± 3.458#	28.162 ± 3.645#
Heart TNF-α levels (ng/g protein)	6.402 ± 0.343	5.768 ± 0.756***	14.787 ± 1.154***	5.925 ± 0.566ε##	5.90 ± 0.346ε#

Note: Statistical analysis was performed using a one-way analysis of variance (ANOVA) followed by the Tukey post hoc test for the analysis of TAS, TOS, and cleaved caspase-3 levels in the liver. Statistical analysis was also performed using a Kruskal–Wallis one-way ANOVA on ranks followed by the Mann–Whitney *U* test for the analysis of OSI and neopterin levels in the liver. All values are mean ± SEM. $n = 6$ for each group.
Abbreviations: CON, control; ENAC-50, EPI + NAC (50 mg/kg); ENAC-300, EPI + NAC (300 mg/kg); EPI, epirubicin; NAC, N-acetylcysteine; OSI, oxidative stress index; TAS, total antioxidant status; TNF-α, tumor necrosis factor-alpha; TOS, total oxidant status.
*$p < 0.05$ vs. CON.
**$p < 0.01$ vs. CON.
***$p < 0.001$ vs. CON.
$p < 0.05$ vs. EPI.
$p < 0.001$ vs. EPI.
$p < 0.000$ vs. EPI.
$p < 0.05$ vs. ENAC-50.

the ENAC-50 and ENAC-300 groups; however, this trend did not reach statistical significance.

3.4 | Hepatic KP-Related Parameters

Hepatic Trp levels were significantly increased in the EPI group (72.765 ± 10.467 ng/g protein) compared to the CON (44.477 ± 4.437 ng/g protein), NAC (44.488 ± 2.909 ng/g protein), ENAC-50, and ENAC-300 (37.901 ± 2.779 ng/g protein) groups ($p = 0.010$, $p = 0.010$, $p = 0.003$, and $p = 0.001$, respectively) (Figure 2A).

Hepatic Kyn levels in the EPI group (1900 ± 211 ng/g protein) were significantly higher compared to the CON group (1319 ± 56.7 ng/g protein) ($p = 0.016$), markedly higher compared to the NAC group (1248 ± 254 ng/g protein), and significantly lower in the ENAC-300 group (904 ± 35 ng/g protein) compared to the CON, EPI, and ENAC-50 (1414 ± 255 ng/g protein) groups ($p = 0.004$, $p = 0.004$, $p = 0.037$) (Figure 2B). The hepatic KYNA levels were measured at 10,071 ± 1654 ng/g protein in the CON group, 9690 ± 1947 ng/g protein in the NAC group, 13,193 ± 1445 ng/g protein in the EPI group, 6358 ± 396 ng/g protein in the ENAC-50 group, and 8418 ± 2893 ng/g protein in the ENAC-300 group. The KYNA levels in the EPI group were significantly higher compared to the ENAC-50 group and noticeably higher than the ENAC-300 group ($p = 0.003$ and $p = 0.060$, respectively) (Figure 2C). Hepatic QA levels in the EPI group (322 ± 33 ng/g protein) were significantly higher than those in the CON group (231 ± 20 ng/g protein), the NAC group (211 ± 14 ng/g protein), the ENAC-50 group (157 ± 14 ng/g protein), and the ENAC-300 group (203 ± 17 ng/g protein) ($p = 0.037$, $p = 0.008$, $p = 0.001$, and $p = 0.004$, respectively) (Figure 2D). Hepatic KMO levels in the EPI group (69,742 ± 7056 ng/g protein) were significantly higher than those in the CON group (48,227 ± 6637 ng/g protein) and the ENAC-300 group (43,289 ± 4403 ng/g protein) and were markedly higher compared to the NAC group (51,257 ± 3361 ng/g protein) and the ENAC-50 group (49,046 ± 4312 ng/g protein) ($p = 0.037$, $p = 0.016$, $p = 0.055$, and $p = 0.078$, respectively) (Figure 3A). Hepatic kynureninase levels in the EPI group (953 ± 124 ng/g protein) were significantly higher than those in the CON group (331 ± 37 ng/g protein), the NAC group (561 ± 49 ng/g protein), the ENAC-50 group (231 ± 55 ng/g protein), and the ENAC-300 group (422 ± 308 ng/g protein) ($p = 0.001$, $p = 0.005$, $p = 0.001$, and

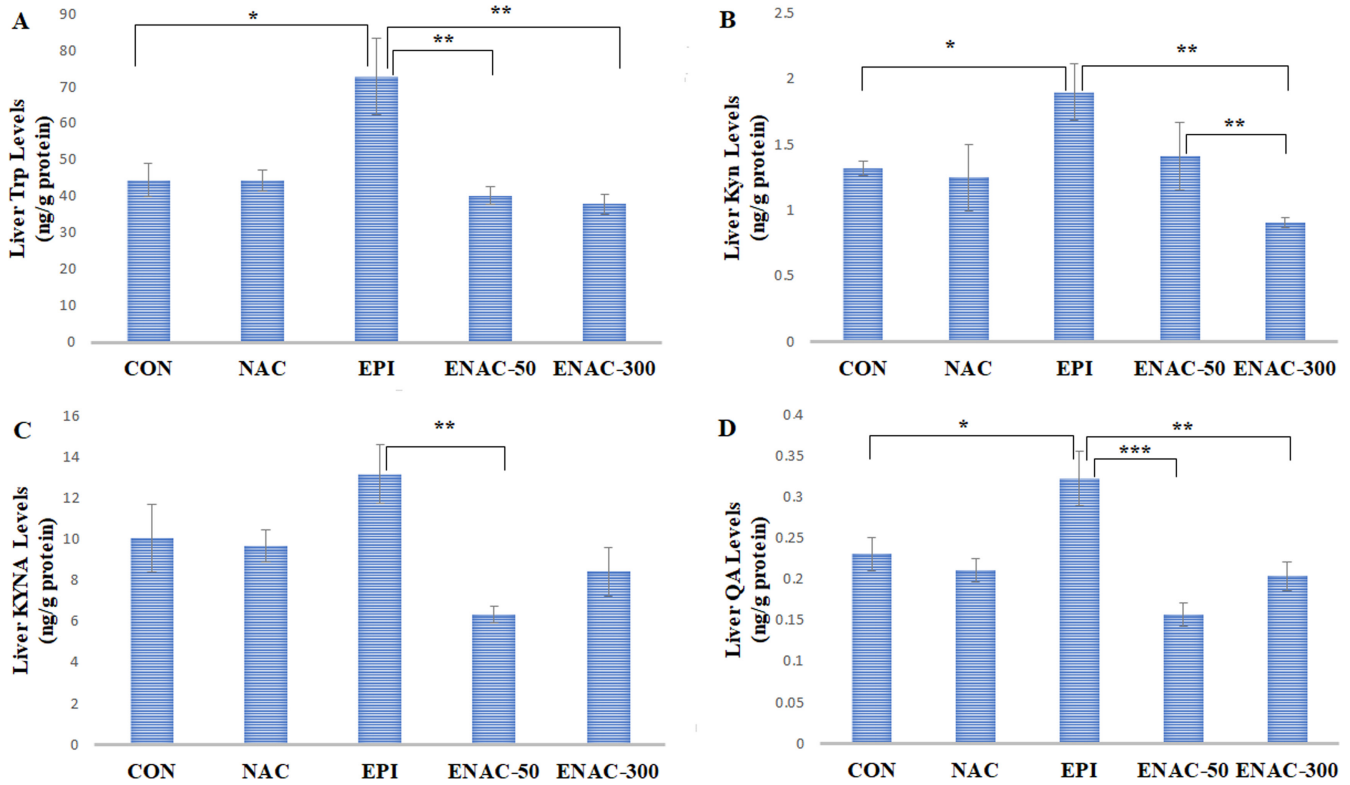

FIGURE 2 | Hepatic levels of KP metabolites. (A) Liver Trp levels; (B) liver Kyn levels; (C) liver KYNA levels; and (D) liver QA levels. Statistical analysis was performed using a one-way analysis of variance (ANOVA) followed by the Tukey post hoc test to analyze Trp levels in the liver tissue and a Kruskal–Wallis one-way ANOVA on ranks followed by the Mann–Whitney *U* test for the analysis of Kyn, KYNA, and QA levels. All values are mean ± SEM. $n = 6$ for each group. *, $p < 0.05$; **, $p < 0.01$; ***, $p < 0.001$. Abbreviations: Kyn, kynurenine; KYNA, kynurenic acid; QA, quinolinic acid; Trp, tryptophan.

$p = 0.001$, respectively) (Figure 3B). No difference was observed between groups in hepatic KTR and QA/KYNA levels (Figure 3C,D).

3.5 | Correlation Result Between KP Metabolites and Biochemical Results

As shown in Table 3, correlation analysis revealed the relationship between liver KMO levels and LDL (Pearson $r = 0.382$, $p = 0.037$), T-chol (Pearson $r = 0.432$, $p = 0.017$), AST/ALT (Pearson $r = 0.411$, $p = 0.024$), CK-MB (Pearson $r = 0.393$, $p = 0.032$), and cleaved caspase-3 (Pearson $r = 0.404$, $p = 0.077$), as well as the relationship between liver QA levels and LDL (Pearson $r = 0.584$, $p = 0.001$), TG (Pearson $r = 0.391$, $p = 0.033$), AST (Pearson $r = 0.368$, $p = 0.046$), AST/ALT (Pearson $r = 0.424$, $p = 0.020$), CK (Spearman $r = 0.380$, $p = 0.038$), CK-MB (Spearman $r = 0.380$, $p = 0.038$), and cleaved caspase-3 (Pearson $r = 0.514$, $p = 0.004$). Also, correlation analysis revealed the relationship between liver Trp levels and LDL (Pearson $r = 0.494$, $p = 0.006$), T-chol (Pearson $r = 0.389$, $p = 0.034$), TG (Pearson $r = 0.564$, $p = 0.001$), AST (Pearson $r = 0.403$, $p = 0.027$), AST/ALT (Pearson $r = 0.525$, $p = 0.003$), CK (Spearman $r = 0.432$, $p = 0.017$), CK-MB (Pearson $r = 0.566$, $p = 0.001$), and cleaved caspase-3 (Pearson $r = 0.665$, $p = 0.000$). These correlations are considered exploratory and may be influenced by differences between experimental groups; therefore, they should be interpreted with caution.

3.6 | Histopathological Analysis

The H&E results for heart tissues are shown in Figure 4. The heart tissues of the CON group had a typical morphological structure, and the NAC group section had the same appearance as the CON group. In the EPI group, irregularly arranged muscle fibers and areas of inflammation were observed. In the EPI-50 group, the damage was significantly reduced compared to the EPI group, and the muscle fibers were found to be more regular. In the EPI-300 group, edema and irregularity in tissue fibers, along with moderate damage, were observed. Histopathological examination scores for heart tissues are presented in Table 4. When the EPI group's damage scores were examined, they were found to be statistically higher than those of the CON and NAC groups ($p < 0.5$). The damage scores in the ENAC-50 and ENAC-300 groups were significantly lower compared to the EPI group ($p < 0.5$); however, there was no significant difference between the ENAC-50 and ENAC-300 groups ($p > 0.5$).

4 | Discussion

4.1 | EPI-Induced Oxidative Stress, Cell Death, and Systemic Catabolic Effects

EPI and other anthracycline chemotherapeutics have been shown to induce oxidative stress and pro-inflammatory responses in cardiac tissue, leading to increased ROS and

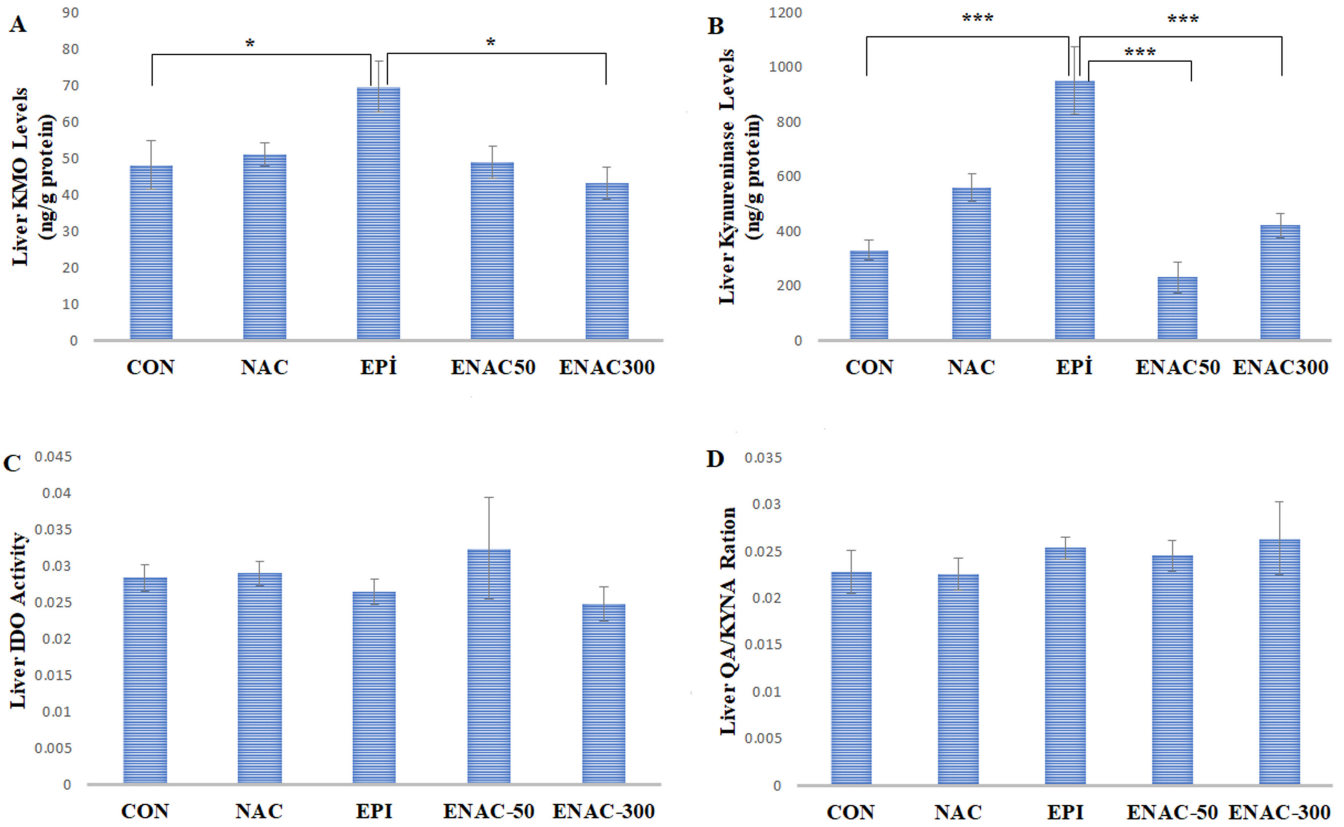

FIGURE 3 | Hepatic expression and enzymatic activity of KP components. (A) Liver KMO levels; (B) liver kynureninase levels; (C) liver KTR levels; and (D) liver QA/KYNA levels. Statistical analysis was performed using a one-way analysis of variance (ANOVA) followed by the Tukey post hoc test to analyze kynureninase levels in the liver tissue and a Kruskal–Wallis one-way ANOVA on ranks followed by the Mann–Whitney *U* test for the analysis of KMO, IDO, and QA/KYNA levels. All values are mean ± SEM. $n = 6$ for each group. *, $p < 0.05$; **, $p < 0.01$; ***, $p < 0.001$. Abbreviations: KMO, Kyn 3-monooxygenase; KTR, kynurenine/tryptophan ratio.

TABLE 3 | Correlation result between KP metabolites and biochemical results.

	KMO		QA		Trp	
	***r* value**	***p* value**	***r* value**	***p* value**	***r* value**	***p* value**
LDL	0.382*	0.037	0.584**	0.001	0.494**	0.006
HDL					−0.026	0.893
T-chol	0.432*	0.017	0.063	0.741	0.389*	0.034
TG	0.111	0.558	0.322	0.083	0.564**	0.001
AST	0.229	0.221	0.391*	0.033	0.403*	0.027
ALT	0.211	0.262	0.368	0.046	0.167	0.379
AST/ALT	0.411	0.024	0.424*	0.020	0.525**	0.003
CK	0.016	0.933	0.380*	0.038	0.432**	0.017
CK-MB	0.393*	0.032	0.380*	0.038	0.566**	0.001
Cleaved caspase-3	0.404*	0.027	0.514**	0.004	0.665***	0.000

Note: Correlation analysis was performed using Pearson's correlation analysis between hepatic KMO levels and LDL, HDL, T-chol, TG, AST, AST/ALT, CK, CK-MB, and cleaved caspase-3 levels; QA levels and LDL, T-chol, TG, AST, AST/ALT, CK-MB, and cleaved caspase-3 levels; and Trp levels and LDL, T-chol, TG, AST, ALT, AST/ALT, CK-MB, and cleaved caspase-3 levels, as well as Spearman's correlation analysis between hepatic QA and CK and CK-MB levels and between hepatic Trp and CK levels. $n = 30$ for each group.
Abbreviations: AST, aspartate aminotransferase; CK, creatine kinase; CK-MB, creatine kinase–MB isoenzyme; KMO, Kyn 3-monooxygenase; LDL, low-density lipoprotein; QA, quinolinic acid; T-chol, total cholesterol; TG, triglyceride; Trp, tryptophan.
*$p < 0.05$.
**$p < 0.01$.
***$p < 0.001$.

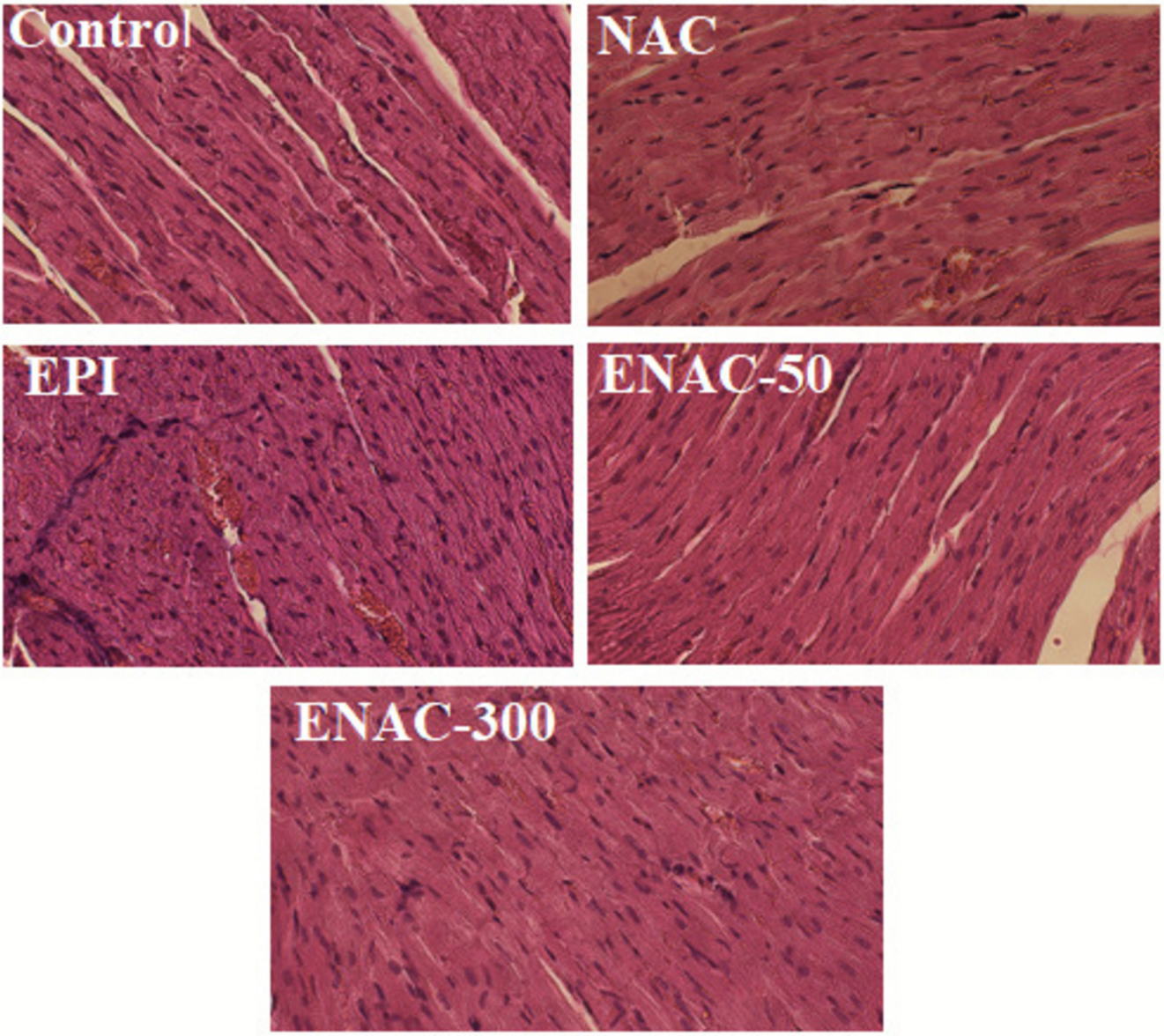

FIGURE 4 | Histological changes in the heart with H&E stain (magnification × 40). Control: The control group displayed a typical structure; NAC: The NAC group had a histological appearance similar to the control group; EPI: The EPI group displayed irregularly arranged muscle fibers and areas of inflammation; ENAC-50: The ENAC-50 group had reduced damage, and the muscle fibers were more regularly arranged; ENAC-300: The ENAC-300 group displayed moderate damage with edema and disorganization of tissue fibers.

TABLE 4 | Histopathological scores of liver injury.

Parameters	Control Median (25–75)	NAC Median (25–75)	EPI Median (25–75)	ENAC-50 Median (25–75)	ENAC-300 Median (25–75)	Test İst.	*p*
Total score	0 (0–1) A	0 (0–1) A	3 (2–3) C	1 (1–2) A	2 (2–3) B	138.539	< 0.001

Note: Statistical analysis was done using a Kruskal–Wallis one-way analysis of variance on ranks. All pairwise multiple comparison procedures were done using the Dunn–Bonferroni post hoc test. All values are mean ± SEM, and $n = 6$ for each group, A < B < C < D; $p < 0.005$.

elevated levels of inflammatory cytokines, including TNF-α, contributing to cardiomyocyte injury and dysfunction (Fabiani et al. 2021). Supporting the existing literature, increased OSI and TNF-α levels were observed in the cardiac tissue of the EPI group in our study, and these biochemical alterations were corroborated by histological evidence of myocardial damage. In addition, plasma CK-MB levels and the AST/ALT ratio, both considered indicators of cardiovascular injury (Higashitani et al. 2022), were reported. In the present study, plasma CK-MB levels and the AST/ALT ratio were significantly increased in the EPI group compared with the CON group. Thus, our findings are consistent with previous

studies, demonstrating that chemotherapeutic agents, particularly anthracyclines such as doxorubicin and EPI, increase cardiac biomarkers (Ding et al. 2024). Moreover, CK-MB release requires loss of membrane integrity (Omran et al. 2022). In apoptosis, cells undergo programmed cell death in a controlled manner without loss of membrane integrity or release of intracellular contents into the extracellular space, resulting in minimal inflammatory response (Erekat 2025). Taken together, the histological and biochemical findings suggest that myocardial injury in the EPI group may predominantly involve apoptosis-independent cell death mechanisms that compromise membrane integrity rather than classical apoptosis. In line with this interpretation, recent studies have shown that EPI induces ferroptosis in cardiomyocytes, a regulated form of cell death closely linked to lipid peroxidation and necrotic-like tissue damage (Erekat 2022).

Interestingly, plasma CK levels were decreased, possibly reflecting reduced muscle mass in the EPI group. Consistent with this view, pronounced body weight loss was observed in EPI-treated animals. Supporting this notion, chemotherapy has been shown to exacerbate skeletal muscle loss in cancer patients through a multifactorial interplay involving treatment-related anorexia, nausea, and generalized physiological stress (Pedrosa et al. 2023; Mallard et al. 2024). Notably, sarcopenia has been identified as a significant risk factor for severe toxicity in patients with breast cancer receiving perioperative EPI therapy (Ueno et al. 2020). Moreover, patients with breast cancer have been reported to exhibit a reduced number of skeletal muscle sarcomeres compared with healthy controls even before the initiation of chemotherapy (Gamble et al. 2023). Collectively, these findings indicate that the catabolic phase is characterized by accelerated proteolysis in skeletal muscle, leading to increased release of amino acids into the circulation and enhanced hepatic uptake and utilization in the liver (Vary et al. 1989). Our results showed increased hepatic Trp levels in the EPI group, and we suggest that increased hepatic Trp levels may be due to increased catabolic processes in skeletal muscle. Moreover, decreased CK levels in the EPI group may be related to skeletal muscle loss.

Supporting this view, decreased CK levels have been reported in patients with type 2 diabetes and low muscle mass, further supporting the association between reduced CK levels and muscle wasting (Hu et al. 2023). Similarly, clinical observations have shown that a subset of patients initially diagnosed with acute myocardial infarction (AMI) presented with low total CK and elevated CK-MB levels. However, total CK subsequently increased in most cases (Vladutiu and Schachner 1989). Taken together, these findings suggest that EPI contributes to cardiac toxicity, consistent with previous reports (Dong et al. 2022). Thus, the reduction in CK levels observed in the EPI group may be related to skeletal muscle loss; however, the effects of EPI on body weight and muscle mass warrant further investigation.

On the other hand, it is well established that hyperlipidemia is a significant risk factor for cardiovascular diseases (Yang et al. 2006). Our results are consistent with previous studies demonstrating that anthracycline-based chemotherapy induces hyperlipidemia, which may be associated with increased oxidative stress, as reflected by an elevated OSI index. Hyperlipidemia has also been linked to hepatic dysfunction, and chemotherapeutic agents are known to affect liver function adversely (Lu et al. 2020; Zhu et al. 2020). In agreement with this evidence, increased plasma lipid levels were observed in the EPI group.

4.2 | Hepatic KP Activation and Interpretation of Liver Injury

Our study demonstrated that KP metabolites, including Kyn, QA, and KYNA, were elevated in the livers of the EPI group, indicating activation of the hepatic KP. The first and rate-limiting step of this pathway is regulated by both IDO and tryptophan 2,3-dioxygenase (TDO). Although inflammatory stimuli and oxidative stress primarily induce IDO, which is widely expressed in extrahepatic tissues, TDO is predominantly expressed in the liver and regulated mainly under physiological and metabolic conditions.

Although inflammatory conditions may induce IDO expression, the KTR—commonly used as a proxy for IDO activity—remained unchanged in our study. This finding does not necessarily exclude IDO involvement, as increased substrate availability, reflected by elevated hepatic Trp levels, may mask changes in IDO activity when assessed by ratio-based indices. Moreover, emerging evidence indicates that both IDO and TDO can be expressed under cancer-related conditions and that tumor or host tissues may utilize either enzyme, or both, to regulate KP metabolism (Obara-Michlewska 2022).

Neopterin has been proposed as a marker linking circulating Trp levels to inflammation-induced IDO activation (Jorgensen et al. 2025). In the present study, the absence of a concomitant increase in neopterin levels, together with the hepatic localization of our measurements and the unchanged KTR, suggests that the observed KP activation in the EPI group may predominantly reflect TDO-mediated regulation rather than classical inflammation-driven IDO activation. Importantly, although changes in downstream metabolites support pathway-level activation of the hepatic KP, they do not allow a definitive distinction between the relative contributions of IDO and TDO at the initial step.

Recent studies have demonstrated that alterations in KP metabolites exert significant immunological effects and are closely associated with the development and progression of various pathological conditions (Jasim et al. 2023; Al-Hakeim et al. 2023; Al-Hakeim et al. 2025). In addition, the balance between KP metabolites influences their pathophysiological roles. In our study, both QA and KYNA levels increased in the liver of the EPI group, without a significant change in the QA/KYNA ratio.

The increase in KYNA may represent a compensatory defense mechanism, as KYNA has been shown to scavenge ROS and exert cytoprotective effects (Han et al. 2021a), unlike QA (Al-Hakeim et al. 2025; Crump et al. 2024). Nevertheless, this potential protective response does not appear sufficient to prevent apoptosis in the liver of the EPI group. These findings suggested that other pro-apoptotic KP metabolites, such as Trp and 3-HK, may contribute to apoptotic signaling. Previous studies have reported that downstream metabolites such as 3-HK possess

pro-apoptotic properties and have also highlighted that KMO is a critical metabolic checkpoint regulating the balance between cytotoxic (3-HK and QA) and cytoprotective (KYNA) branches of the KP. Inhibition of KMO has been shown to attenuate the production of 3-HK and QA, thereby shifting KP away from the oxidative, cytotoxic branch (Al-Hakeim et al. 2023; Kupjetz et al. 2025). Accordingly, the increased KMO expression and elevated QA levels observed in the EPI group may suggest activation of the apoptosis-related downstream branch of the KP. Supporting this interpretation, cleaved caspase-3 levels correlated positively with hepatic Trp, KMO, and QA levels in the EPI group. However, as 3-HK levels were not directly measured, these findings do not demonstrate accumulation of 3-HK per se. Thus, our results are interpreted as reflecting activation of the KP rather than the accumulation of a specific intermediate metabolite and are presented within a hypothesis-generating framework.

Although apoptosis was increased in the liver of the EPI group, plasma ALT levels did not increase, suggesting that necrotic cell death and membrane disruption are required for ALT release into the circulation (Han, Ryu, et al. 2021b). Because disruption of the cell membrane is required for the release of intracellular enzymes into the plasma, also supporting this, plasma AST levels have been shown to correlate with the extent of necrosis in hepatic ischemia–reperfusion models (Yang et al. 2014; O'Brien et al. 2000). Furthermore, reduced KMO levels have been reported in patients with pancreatic necrosis (Jakkampudi et al. 2023).

Therefore, our results suggest that the increased hepatic KMO levels observed in the EPI-treated group may be associated with relative suppression of necrotic cell death, which could partly explain the absence of elevated plasma ALT levels.

Beyond liver injury, our results suggest that alterations in KP metabolites may be indirectly associated with hepatic detoxification capacity and may contribute to EPI-induced cardiac toxicity. The liver is the primary site of anthracycline metabolism, and dose adjustment is recommended in patients with impaired liver function (Kebieche et al. 2009). Clinical pharmacokinetic studies have demonstrated that hepatic clearance of EPI correlates with serum AST levels, and elevated AST has been associated with reduced EPI clearance and increased systemic toxicity (Fabbi et al. 2015; Twelves et al. 1992).

Similarly, metabolomic analyses in anthracycline-induced liver injury models have revealed close associations between AST/ALT levels and hepatic metabolic disturbances, and antioxidant treatment has been shown to ameliorate both liver enzyme elevations and cardiac injury, highlighting a functional hepatocardiac interaction (Aikemu et al. 2016). In clinical practice, combined liver function parameters, including AST/ALT ratios, are increasingly recommended for monitoring suspected drug-induced liver injury (Treem et al. 2021). Thus, AST may serve as a sensitive indicator reflecting changes in EPI pharmacokinetics. In addition, QA accumulation has been reported to reflect the severity of liver dysfunction (Chen et al. 2021), and Trp-derived metabolites have been shown to modulate cytochrome P450 expression, thereby influencing xenobiotic metabolism, immune responses, and cellular homeostasis (Haduch et al. 2023). These findings suggest that alterations in the hepatic KP may underlie hepatic dysfunction observed during chemotherapeutic interventions.

In the present study, positive correlations were observed between plasma CK-MB levels and AST/ALT ratios, as well as hepatic KMO expression and Trp and QA levels, suggesting a potential link between hepatic KP activation and cardiac injury. Moreover, plasma LDL and T-chol levels correlated positively with hepatic Trp, QA, and KMO levels. Elevated plasma lipid parameters have been linked to hepatic dysfunction (Kathak et al. 2022), and mechanistic studies indicate that upregulation of IDO may contribute to dyslipidemia (Wang et al. 2025). Therefore, our results suggest that the observed correlations among plasma CK-MB levels, AST/ALT ratios, hepatic KMO expression, and Trp and QA levels may indicate an interaction among KP activation, altered hepatic metabolic function, and cardiac injury. However, these associations are exploratory and hypothesis-generating and should be interpreted with caution. Further studies incorporating direct pharmacokinetic and hepatic clearance assessments are warranted to clarify this relationship.

4.3 | Dose-Dependent Effects of NAC and the Hepato-Cardiac Axis

In our study, NAC administration improved plasma lipid and cardiac parameters in the ENAC-50 and ENAC-300 groups. Supporting NAC's lipid-lowering effects, Yang et al. (2006) reported that in rats fed a high-fat diet (HFD), a weakened antioxidant defense system led to hyperlipidemia; NAC partially reversed these changes. Additionally, in experimental models, NAC has been shown to improve plasma lipid profiles and restore redox balance under dyslipidemic conditions, thereby enhancing myocardial protection and reducing infarct size in settings of ischemia–reperfusion injury and HFD-induced oxidative stress (Zaobornyj et al. 2025). Thus, our findings suggest that NAC's lipid-lowering effects may contribute to its cardioprotective properties.

In addition, NAC administration decreased the OSI index, cleaved caspase-3 levels, and KMO expression in the liver of the ENAC-50 group and normalized hepatic Trp levels in this group. Thus, it can be concluded that EPI activates an adaptive mechanism in liver tissue via the KP pathway and that NAC application can normalize these parameters. However, it is essential to consider the dose-dependent effects of NAC supplementation, as high doses can be toxic and even cause cell death or apoptosis (Liu et al. 2017). In the present study, the OSI index was increased in the liver of the ENAC-300 group; however, this increase did not result in significant changes in the assessed biochemical parameters. This observation may be related to the administration of high-dose NAC, which has been reported to attenuate antioxidant capacity and thereby contribute to oxidative stress paradoxically. NAC mainly acts by regulating the supply of cysteine for glutathione (GSH) synthesis. However, mechanistic research also indicates that high-dose NAC administration can reduce GSH levels and may lead to oxidative stress (Tenório et al. 2021; Devrim-Lanpir et al. 2021; Mlejnek et al. 2021). Moreover, the ENAC-50 group showed reduced OSI

and TNF-α levels in cardiac tissue, accompanied by improved myocardial morphology; the ENAC-300 group did not demonstrate further improvement in these parameters. Collectively, these findings suggest that the biological effects of NAC under EPI-induced toxicity may not be linearly dose dependent and that higher doses may shift the redox equilibrium toward a less favorable state. Nevertheless, the underlying mechanisms and the dose-dependent profile of NAC require further investigation.

5 | Conclusion

This study suggests that EPI administration activates the hepatic KP, disrupts lipid metabolism, and induces oxidative stress and apoptosis, which may collectively contribute to impaired hepatic clearance and cardiotoxicity. NAC supplementation, particularly at a moderate dose, effectively ameliorated these alterations by reducing oxidative damage and modulating KP-related enzyme activity. These findings highlight the role of KP metabolites, especially Trp, QA, and KMO, as potential mediators of chemotherapy-related toxicity. Targeting the KP pathway may be a promising strategy to mitigate EPI-induced adverse effects and improve treatment outcomes.

Author Contributions

E.A. designed the study and performed biochemical and statistical analyses. I.E. performed histological analyses. E.A. and M.Ö. conducted the literature review and interpreted the analysis results.

Funding

The authors have nothing to report.

Conflicts of Interest

The authors declare no conflicts of interest.

Data Availability Statement

The data that support the findings of this study are available from the corresponding author upon reasonable request.

References

Aikemu, A., N. Amat, A. Yusup, L. Shan, X. Qi, and H. Upur. 2016. "Attenuation Effect of Abnormal Savda Munziq on Liver and Heart Toxicity Caused by Chemotherapy in Mice." *Experimental and Therapeutic Medicine* 12, no. 1: 384–390.

Al-Hakeim, H. K., A. K. Abed, S. R. Moustafa, A. F. Almulla, and M. Maes. 2023. "Tryptophan Catabolites, Inflammation, and Insulin Resistance as Determinants of Chronic Fatigue Syndrome and Affective Symptoms in Long COVID." *Frontiers in Molecular Neuroscience* 16: 1194769.

Al-Hakeim, H. K., A. A. R. Al-Issa, C. Chen, and M. Maes. 2025. "The Tryptophan Catabolite Pathway in Major and Simple Neurocognitive Psychosis: A Double-Edged Sword With Two Sharpened Edges." *Acta Neuropsychiatrica*: 1–30. https://doi.org/10.1017/neu.2025.5.

Alves, A. C., D. Ribeiro, C. Nunes, and S. Reis. 2016. "Biophysics in Cancer: The Relevance of Drug-Membrane Interaction Studies." *Biochimica et Biophysica Acta* 1858, no. 9: 2231–2244.

Ayala, T. B., D. R. R. Ortega, P. O. O. Rodríguez, et al. 2021. "Subchronic N-Acetylcysteine Treatment Decreases Brain Kynurenic Acid Levels and Improves Cognitive Performance in Mice." *Antioxidants* 10, no. 2: 147.

Bekki, K., H. Vogel, W. Li, et al. 2015. "The Aryl Hydrocarbon Receptor (AhR) Mediates Resistance to Apoptosis Induced in Breast Cancer Cells." *Pesticide Biochemistry and Physiology* 120: 5–13.

Berk, M., O. M. Dean, S. M. Cotton, et al. 2014. "The Efficacy of Adjunctive N-Acetylcysteine in Major Depressive Disorder: A Double-Blind, Randomized, Placebo-Controlled Trial." *Journal of Clinical Psychiatry* 75, no. 6: 628–636.

Blanco-Ayala, T., K. V. Sathyasaikumar, J. D. Uys, V. Pérez-de-la-Cruz, L. S. Pidugu, and R. Schwarcz. 2020. "N-Acetylcysteine Inhibits Kynurenine Aminotransferase II." *Neuroscience* 444: 160–169.

Bradford, M. M. 1976. "A Rapid and Sensitive Method for the Quantitation of Microgram Quantities of Protein Utilizing the Principle of Protein-Dye Binding." *Analytical Biochemistry* 72: 248–254.

Chen, S. S., Y. Huang, Y. M. Guo, et al. 2021. "Serum Metabolomic Analysis of Chronic Drug-Induced Liver Injury With or Without Cirrhosis." *Frontiers in Medicine* 8: 8.

Crump, L. S., J. L. Floyd, L. W. Kuo, et al. 2024. "Targeting Tryptophan Catabolism in Ovarian Cancer to Attenuate Macrophage Infiltration and PD-L1 Expression." *Cancer Research Communications* 4, no. 3: 822–833.

Devaleriola, D. 1994. "Dose Optimization of Anthracyclines." *Anticancer Research* 14, no. 6a: 2307–2313.

Devrim-Lanpir, A., L. Hill, and B. Knechtle. 2021. "How N-Acetylcysteine Supplementation Affects Redox Regulation, Especially at Mitohormesis and Sarcohormesis Level: Current Perspective." *Antioxidants* 10, no. 2: 153.

Ding, S. S., S. Xiong, X. Wang, et al. 2024. "Effects of Doxorubicin, Epirubicin, and Liposomal Doxorubicin (Anthracycline) on Cardiac Function in Patients With Osteosarcoma and Their Influencing Factors." *Clinical & Translational Oncology* 26, no. 6: 1459–1466.

Dobbs, N. A., C. J. Twelves, W. Gregory, C. Cruickshanka, M. A. Richards, and R. D. Rubens. 2003. "Epirubicin in Patients With Liver Dysfunction: Development and Evaluation of a Novel Dose Modification Scheme." *European Journal of Cancer* 39, no. 5: 580–586.

Dobbs, N. A., C. J. Twelves, P. Rizzi, et al. 1994. "Epirubicin in Hepatocellular Carcinoma: Pharmacokinetics and Clinical Activity." *Cancer Chemotherapy and Pharmacology* 34, no. 5: 405–410.

Dong, Z. Y., Z. Liu, S. Chen, C. Zhang, J. Xiao, and X. Zhou. 2022. "Cardiovascular Status of Breast Cancer Patients Before and After Receiving Anthracycline Chemotherapy Regimen." *Nursing Open* 9, no. 1: 256–266.

Dur, A., H. Kose, A. Kocyigit, O. Kocaman, M. Ismayilova, and F. C. Sonmez. 2016. "The Anti-Inflammatory and Antioxidant Effects of Thymoquinone on Ceruleine Induced Acute Pancreatitis in Rats." *Bratislavské Lekárske Listy* 117, no. 10: 614–618.

Erekat, N. S. 2022. "Programmed Cell Death in Diabetic Nephropathy: A Review of Apoptosis, Autophagy, and Necroptosis." *Medical Science Monitor* 28: e937766.

Erekat, N. S. 2025. "Programmed Cell Death and Its Therapeutic Implications in Parkinson's Disease: A Review of Apoptosis, Autophagy, Ferroptosis, and Necroptosis." In *Clinical Anatomy*.

Fabbi, P., P. Spallarossa, S. Garibaldi, et al. 2015. "Doxorubicin Impairs the Insulin-Like Growth Factor-1 System and Causes Insulin-Like Growth Factor-1 Resistance in Cardiomyocytes." *PLoS ONE* 10, no. 5: e0124643.

Fabiani, I., A. Aimo, C. Grigoratos, et al. 2021. "Oxidative Stress and Inflammation: Determinants of Anthracycline Cardiotoxicity and Possible Therapeutic Targets." *Heart Failure Reviews* 26, no. 4: 881–890.

Gamble, D. T., J. Ross, H. Khan, et al. 2023. "Impaired Cardiac and Skeletal Muscle Energetics Following Anthracycline Therapy for Breast Cancer." *Circulation. Cardiovascular Imaging* 16, no. 10: e015782.

Haduch, A., E. Bromek, W. Kuban, and W. A. Daniel. 2023. "The Engagement of Cytochrome P450 Enzymes in Tryptophan Metabolism." *Metabolites* 13, no. 5: 629.

Han, J., J. Zhang, and C. L. Zhang. 2021a. "Irinotecan-Induced Steatohepatitis: Current Insights." *Frontiers in Oncology* 11: 754891.

Han, M., G. Ryu, S. A. Shin, et al. 2021b. "Physiological Roles of Apoptotic Cell Clearance: Beyond Immune Functions." *Life (Basel)* 11, no. 11: 1141.

Higashitani, M., A. Mizuno, T. Kimura, et al. 2022. "Low Aspartate Aminotransferase (AST)/Alanine Aminotransferase (ALT) Ratio Associated With Increased Cardiovascular Disease and Its Risk Factors in Healthy Japanese Population." *Journal of Gastrointestinal and Liver Diseases* 31, no. 4: 429–436.

Hu, W. C., Y. Ma, L. He, and D. Xing. 2023. "The Correlation Between Serum Creatine Kinase With Low Muscle Mass in Type 2 Diabetes Patients." *Journal of Investigative Medicine* 71, no. 3: 279–285.

Jakkampudi, A., P. Sarkar, M. Unnisa, et al. 2023. "Kynurenine Pathway Alteration in Acute Pancreatitis and Its Role as a Biomarker of Infected Necrosis." *Pancreatology* 23, no. 6: 589–600.

Jasim, Z. A., H. K. al-Hakeim, S. Zolghadri, and A. Stanek. 2023. "Maternal Tryptophan Catabolites and Insulin Resistance Parameters in Preeclampsia." *Biomolecules* 13, no. 10: 1447.

Jorgensen, S. F., P. R. Braadland, T. Ueland, et al. 2025. "Tryptophan-Kynurenine Metabolites Associate With Inflammation and Immunologic Phenotypes in Common Variable Immunodeficiency." *Journal of Allergy and Clinical Immunology* 156, no. 3: 814–824.e11.

Kalimeris, K., P. Briassoulis, A. Ntzouvani, et al. 2016. "N-Acetylcysteine Ameliorates Liver Injury in a Rat Model of Intestinal Ischemia Reperfusion." *Journal of Surgical Research* 206, no. 2: 263–272.

Kathak, R. R., A. H. Sumon, N. H. Molla, et al. 2022. "The Association Between Elevated Lipid Profile and Liver Enzymes: A Study on Bangladeshi Adults." *Scientific Reports* 12, no. 1: 1771.

Kebieche, M., Z. Lakroun, M. Lahouel, J. Bouayed, Z. Meraihi, and R. Soulimani. 2009. "Evaluation of Epirubicin-Induced Acute Oxidative Stress Toxicity in Rat Liver Cells and Mitochondria, and the Prevention of Toxicity Through Quercetin Administration." *Experimental and Toxicologic Pathology* 61, no. 2: 161–167.

Kupjetz, M., T. Y. Wences Chirino, N. Joisten, and P. Zimmer. 2025. "Kynurenine Pathway Dysregulation as a Mechanistic Link Between Cognitive Impairment and Brain Damage: Implications for Multiple Sclerosis." *Brain Research* 1853: 149415.

Liu, Y., K. Liu, N. Wang, and H. Zhang. 2017. "N-Acetylcysteine Induces Apoptosis via the Mitochondria-Dependent Pathway but Not via Endoplasmic Reticulum Stress in H9c2 Cells." *Molecular Medicine Reports* 16, no. 5: 6626–6633.

Lu, Q., X. Wu, Y. Zhu, et al. 2020. "Effects of Chemotherapy on Serum Lipids in Chinese Postoperative Breast Cancer Patients." *Cancer Management and Research* 12: 8397–8408.

Mallard, J., E. Hucteau, L. Bender, et al. 2024. "A Single Chemotherapy Administration Induces Muscle Atrophy, Mitochondrial Alterations and Apoptosis in Breast Cancer Patients." *Journal of Cachexia, Sarcopenia and Muscle* 15, no. 1: 292–305.

Mlejnek, P., P. Dolezel, E. Kriegova, and N. Pastvova. 2021. "N-Acetylcysteine Can Induce Massive Oxidative Stress, Resulting in Cell Death With Apoptotic Features in Human Leukemia Cells." *International Journal of Molecular Sciences* 22, no. 23: 12635.

Obara-Michlewska, M. 2022. "The Tryptophan Metabolism, Kynurenine Pathway and Oxidative Stress-Implications for Glioma Pathobiology." *Neurochemistry International* 158: 105363.

O'Brien, T., G. Babcock, J. Cornelius, et al. 2000. "A Comparison of Apoptosis and Necrosis Induced by Hepatotoxins in HepG2 Cells." *Toxicology and Applied Pharmacology* 164, no. 3: 280–290.

Omran, F., I. Kyrou, F. Osman, V. G. Lim, H. S. Randeva, and K. Chatha. 2022. "Cardiovascular Biomarkers: Lessons of the Past and Prospects for the Future." *International Journal of Molecular Sciences* 23, no. 10: 5680.

Ozturk, E., O. Balat, Y. G. Acılmıs, C. Ozcan, S. Pence, and Ö. Erel. 2011. "Measurement of the Placental Total Antioxidant Status in Preeclamptic Women Using a Novel Automated Method." *Journal of Obstetrics and Gynaecology Research* 37, no. 4: 337–342.

Pedrosa, M. B., S. Barbosa, R. Vitorino, R. Ferreira, D. Moreira-Gonçalves, and L. L. Santos. 2023. "Chemotherapy-Induced Molecular Changes in Skeletal Muscle." *Biomedicine* 11, no. 3: 905.

Periyanayagam, S., G. Arumugam, A. Ravikumar, and V. S. Ganesan. 2015. "Thymoquinone Ameliorates NLRP3-Mediated Inflammation in the Pancreas of Albino Wistar Rats Fed Ethanol and High-Fat Diet." *Journal of Basic and Clinical Physiology and Pharmacology* 26, no. 6: 623–632.

Petit, K., M. Suwalsky, J. R. Colina, et al. 2020. "Toxic Effects of the Anticancer Drug Epirubicin In Vitro Assayed in Human Erythrocytes." *Toxicology In Vitro* 68: 104964.

Sabbaghziarani, F., P. Soleimani, F. R. Eynshikh, F. Zafari, and E. Aali. 2024. "Reduced Ischemia-Reperfusion Oxidative Stress Injury by Melatonin and N-Acetylcysteine in the Male Rat Brain." *IBRO Neuroscience Reports* 17: 131–137.

Tan, Q. W., S. H. Deng, and L. J. Xiong. 2025. "Role of Kynurenine and Its Derivatives in Liver Diseases: Recent Advances and Future Clinical Perspectives." *International Journal of Molecular Sciences* 26, no. 3: 968.

Tenório, M. C. D., N. G. Graciliano, F. A. Moura, A. C. M. de Oliveira, and M. O. F. Goulart. 2021. "*N*-Acetylcysteine (NAC): Impacts on Human Health." *Antioxidants* 10, no. 6: 967.

Treem, W. R., M. Palmer, I. Lonjon-Domanec, et al. 2021. "Consensus Guidelines: Best Practices for Detection, Assessment and Management of Suspected Acute Drug-Induced Liver Injury During Clinical Trials in Adults With Chronic Viral Hepatitis and Adults With Cirrhosis Secondary to Hepatitis B, C and Nonalcoholic Steatohepatitis." *Drug Safety* 44, no. 2: 133–165.

Twelves, C. J., N. A. Dobbs, Y. Michael, et al. 1992. "Clinical Pharmacokinetics of Epirubicin: The Importance of Liver Biochemistry Tests." *British Journal of Cancer* 66, no. 4: 765–769.

Twelves, C. J., S. M. O'Reilly, R. E. Coleman, M. A. Richards, and R. D. Rubens. 1989. "Weekly Epirubicin for Breast-Cancer With Liver Metastases and Abnormal Liver Biochemistry." *British Journal of Cancer* 60, no. 6: 938–941.

Ueno, A., K. Yamaguchi, M. Sudo, and S. Imai. 2020. "Sarcopenia as a Risk Factor of Severe Laboratory Adverse Events in Breast Cancer Patients Receiving Perioperative Epirubicin Plus Cyclophosphamide Therapy." *Supportive Care in Cancer* 28, no. 9: 4249–4254.

Vary, T. C., J. H. Siegel, R. Placko, B. D. Tall, and J. G. Morris. 1989. "Effect of Dichloroacetate on Plasma and Hepatic Amino Acids in Sterile Inflammation and Sepsis." *Archives of Surgery* 124, no. 9: 1071–1077.

Vladutiu, A. O., and A. Schachner. 1989. "Increased Creatine Kinase (CK) MB Isoenzyme in Patients With "Normal" Total CK Activity Suspected of Acute Myocardial Infarction." *Journal of Medicine* 20, no. 1: 73–81.

Wang, D., D. Li, Y. Zhang, et al. 2021. "Functional Metabolomics Reveal the Role of AHR/GPR35 Mediated Kynurenic Acid Gradient Sensing in Chemotherapy-Induced Intestinal Damage." *Acta Pharmaceutica Sinica B* 11, no. 3: 763–780.

Wang, Y., Y. Wu, H. Jiang, et al. 2025. "L-Kynurenine Activates the AHR-PCSK9 Pathway to Mediate the Lipid Metabolic and Ovarian Dysfunction in Polycystic Ovary Syndrome." *Metabolism* 168: 156238.

Yang, M., D. J. Antoine, J. L. Weemhoff, et al. 2014. "Biomarkers Distinguish Apoptotic and Necrotic Cell Death During Hepatic Ischemia/Reperfusion Injury in Mice." *Liver Transplantation* 20, no. 11: 1372–1382.

Yang, R. L., G. le, A. Li, J. Zheng, and Y. Shi. 2006. "Effect of Antioxidant Capacity on Blood Lipid Metabolism and Lipoprotein Lipase Activity of Rats Fed a High-Fat Diet." *Nutrition* 22, no. 11–12: 1185–1191.

Zaobornyj, T., V. Perez, G. Ossani, et al. 2025. "N-Acetylcysteine Treatment Restores the Protective Effect of Heart Ischemic Postconditioning in a Murine Model in the Early Stages of Atherosclerosis." *Pharmaceuticals (Basel)* 18, no. 7: 1014.

Zhu, Y., L. Xiaoan, L. Qi, et al. 2020. "Effects of Chemotherapy on Serum Lipids in Chinese Postoperative Breast Cancer Patients." *European Journal of Cancer* 138: S57.